Hindawi Publishing Corporation
Mathematical Problems in Engineering
Volume 2014, Article ID 130274, 11 pages
http://dx.doi.org/10.1155/2014/130274

Research Article

A Damage Prognosis Method of Girder Structures Based on Wavelet Neural Networks

Rumian Zhong,[1] Zhouhong Zong,[1] Jie Niu,[1,2] and Sujing Yuan[1]

[1] *School of Civil Engineering, Southeast University, Nanjing 210096, China*
[2] *College of EMPS, University of Exeter, Exeter EX4 4QF, UK*

Correspondence should be addressed to Zhouhong Zong; zongzh@seu.edu.cn

Received 21 December 2013; Revised 27 February 2014; Accepted 27 February 2014; Published 6 April 2014

Academic Editor: Ying Lei

Based on the basic theory of wavelet neural networks and finite element model updating method, a basic framework of damage prognosis method is proposed in this paper. Firstly, a damaged I-steel beam model testing is used to verify the feasibility and effectiveness of the proposed damage prognosis method. The results show that the predicted results of the damage prognosis method and the measured results are very well consistent, and the maximum error is less than 5%. Furthermore, Xinyihe Bridge in the Beijing-Shanghai Highway is selected as the engineering background, and the damage prognosis is conducted based on the data from the structural health monitoring system. The results show that the traffic volume will increase and seasonal differences will decrease in the next year and a half. The displacement has a slight increase and seasonal characters in the critical section of mid span, but the strain will increase distinctly. The analysis results indicate that the proposed method can be applied to the damage prognosis of girder bridge structures and has the potential for the bridge health monitoring and safety prognosis.

1. Introduction

Currently, Structural Health Monitoring (SHM) systems are widely used in bridge monitoring and maintenance management. However, they focus on the data accumulation, safety assessment, and so forth. Then the SHM systems can not satisfy the demands of proprietors, because they are generally limited to the damage detection (DD) level, in which the damage in a structural or mechanical system is herein defined as intentional or unintentional changes to its material and/or geometric properties, including variations of its boundary conditions, which adversely affect its performance [1]. According to Farrar et al. and Inman et al. [2–4], damage prognosis (DP) is the theme of future structural health monitoring and can be defined as the estimate of a system's remaining useful life. In other words, damage prognosis attempts to forecast the performance of a system by assessing its current state of damage through NDE measurements, by estimating the future loading environments for that system, and by predicting through simulation and past experience its remaining useful life. The damage prognosis problem includes three main critical areas: (i) sensing and processing hardware, (ii) data interrogation, and (iii) modeling and simulation. The essential differences between DP and DD can be distinguished as follows: DD can only find out the existing damage; on the other hand, DP can predict damage which will occur and its consequences. However, DP is more practical than DD, and its successful implementation will allow the owners to take the necessary protections and maintenances in time to avoid the catastrophic failures, rather than waiting until the occurrence of structural damage or failure [5].

The structural uncertainty and prognosis reliability are the basic topics of DP. Current prognosis methods for predicting structural failures are classified as conventional reliability models, model-based prognosis models, and data-driven prognosis model [3, 6, 7]. The conventional reliability models are used in complex engineering systems, such as rotating machinery [8] and aircraft structures [9, 10]. A physical-based prognostics model begins by constructing a finite element model, and then it is verified or validated using structural monitoring information, and these information along with outputs from the physics-based models will be used to assess

the current state of the structure (e.g., existence, location, and type and extent of damage), which has been proved to predict effectively [11–15]. For most structural applications, physics-based models may not be the most practical solution since the fault type in question is often not unique from component to component. However, physics-based models may be the most suitable approach for cost-justified applications in which accuracy outweighs most other factors and physics models remain consistent across structural systems, such as bridge structures. They also generally require less data than data-driven models.

Data-driven approaches attempt to derive models directly from routinely collecting condition-monitored (CM) data instead of building models based on comprehensive system physics and human expertise. They are built based on historical records and produce prediction outputs directly in terms of CM data [16], including the DP methods based on wavelet artificial neural network [17], Bayesian framework [18–20], Kalman estimator [21, 22], fuzzy theory [23], and probability analysis [24, 25]. The DP methods based on data-driven can detect the structural damage with limited input and output measurement signals; however, the integrity of the data cannot be guaranteed. The wavelet artificial neural network method, which combines denoising ability of wavelet analysis and forecasting ability of neural network, is a fast and rapidly convergent iterative optimization algorithm, and it is widely used in various fields [26–29].

In this paper, the theoretical basis of wavelet neural network algorithm and its implementation process are described. Then, the wavelet neural network method and model updating method are combined to conduct the DP of structure. Subsequently, the framework of DP is proposed and applied to the DP of a damaged I-steel beam and six-span continuous beam bridge, which means the initial realization of the second step of DP-predicting the future structural loads and structural properties. It also laid a solid foundation to the realization of the third step-predicting the remaining life of the structure.

2. The Wavelet Neural Networks

2.1. The Wavelet Neural Networks Model. Many problems are nonlinear in the field of civil engineering. The relationships between variables are so complicated that a large number of practical engineering problems are difficult to have exact solutions in math. However, the wavelet neural networks model is relying on an artificial intelligence algorithm, which uses wavelet unit to replace neuron. The model is composed of many interconnected wavelet units, which are used to simulate the formal structure of the human mind. Then the nonlinear dynamical system based on wavelet network can be obtained. Due to the learning ability, the weight parameters of the network can be updated continuously according to the setting rules, and then the wavelet neural network has the abilities of fitting function and dealing with information [30, 31].

A wavelet neural networks model is shown in Figure 1; it has n nodes in the input layer, l nodes in hidden layer, and

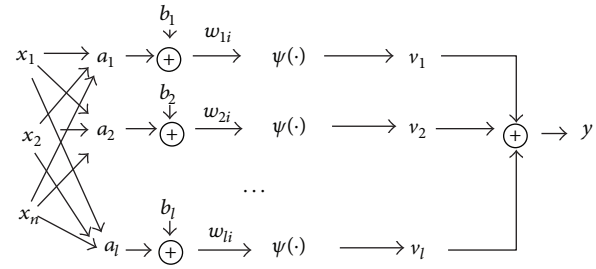

Figure 1: The wavelet neural network model.

only one in the output layer; the network topology is n-l-1, in which the relationship between the inputs and output can be expressed as

$$y = \sum_{k=1}^{l} \nu_k \psi_k = \sum_{k=1}^{l} \nu_k \psi\left(\frac{\sum_{i=1}^{n} w_{ki} x_i - b_k}{a_k}\right), \tag{1}$$

where x_i is the input value of the wavelet neural network; w_{ki} is the weight function between the kth neuron in hidden layer and the ith unit in input layer; ν_k is the weight parameter between the kth neuron in hidden layer and the unit in output layer; $\psi(\cdot)$ is the excitation function of wavelet function; a_k and b_k are the scaling and translation parameters; y is the output value of wavelet neural network.

2.2. A Learning Algorithm of Wavelet Neural Network. The learning algorithm is the core of wavelet neural network, and its purpose is to establish mapping relationship between inputs and outputs by function fitting. A widely applied iterative algorithm called Stochastic Gradient Algorithm (e.g., [26, 32]) is introduced in this paper.

2.2.1. Principle of the Stochastic Gradient Algorithm. A learning sample is given as $(x_{1s}, x_{2s}, \ldots, x_{is}, \ldots, x_{ns}, d_s)$, where the parameter i is the vector components serial number of input value, the parameter s is the learning sample serial number, and d_s is the expected value. Setting y_s as the actual output corresponding to the inputs $(x_{1s}, x_{2s}, \ldots, x_{ns})$, the error function E of the wavelet neural network can be defined as follows:

$$\begin{aligned} E &= \frac{1}{2}\sum_{s=1}^{S}(y_s - d_s)^2 \\ &= \frac{1}{2}\sum_{s=1}^{S}\left(\sum_{k=1}^{l} \nu_k \psi\left(\frac{\sum_{i=1}^{n} w_{ki} x_{is} - b_k}{a_k}\right) - d_s\right)^2. \end{aligned} \tag{2}$$

The principle of wavelet neural network is to get the minimum of E by updating the parameters of wavelet neural network, and then the output y_s which is obtained by fitting can be approximately employed as mapping function to contact inputs and outputs.

2.2.2. The Learning Algorithm. As shown in (1) and (2), the network parameters can be solved based on the Stochastic Gradient Algorithm, and they can be calculated as follows:

$$\begin{aligned} w_{ki} &= w_{ki} + \alpha \Delta w_{ki} \quad i = 1, 2, \ldots, n;\ k = 1, 2, \ldots, l, \\ \nu_k &= \nu_k + \beta \Delta \nu_k \quad k = 1, 2, \ldots, l, \\ a_k &= a_k + \gamma \Delta a_k \quad k = 1, 2, \ldots, l, \\ b_k &= b_k + \eta \Delta b_k \quad k = 1, 2, \ldots, l, \end{aligned} \tag{3}$$

where $\alpha, \beta, \gamma, \eta$ are learning rates. For simplicity,

$$u = \frac{\sum_{i=1}^{n} w_{ki} x_{is} - b_k}{a_k}. \tag{4}$$

Then,

$$\begin{aligned} \Delta w_{ki} &= \frac{\partial E}{\partial w_{ki}} = (y - d) \left(\sum_{k=1}^{l} \nu_k \psi'(u) \right) \frac{x_{is}}{a_k} \\ \Delta \nu_k &= \frac{\partial E}{\partial \nu_k} = (y - d) \left(\sum_{k=1}^{l} \psi(u) \right) \\ \Delta a_k &= \frac{\partial E}{\partial a_k} = (y - d) \left(\sum_{k=1}^{l} \nu_k \psi'(u) \right) \left(-\frac{u}{a_k} \right) \\ \Delta b_k &= \frac{\partial E}{\partial b_k} = (y - d) \left(\sum_{k=1}^{l} \nu_k \psi'(u) \right) \frac{-1}{a_k}, \end{aligned} \tag{5}$$

where $\psi'(u)$ is the first derivative of $\psi(u)$, and then the calculated error, relative error, and the new network parameters can be obtained analytically by substituting (3) into (5). If the relative error can meet the requirements of calculation, the output value will be the optimal solution. The calculation process can be summarized as in Figure 2.

2.2.3. Wavelet Networks and Their Parameterizations

(1) *The Excitation Functions of Wavelet Neural Network.* There are various wavelet functions, such as Harr wavelet, Mever wavelet, Mever Daubechies wavelet, Morlet wavelet, and spline wavelet. Due to the flexibility of choices, there is no uniform standard. Morlet wavelet is a Gaussian wave, and it is widely used and allows adjustment of the relative resolution in time and scale [33, 34]. Morlet wavelet basis function (e.g., [35]) is chosen as the excitation function of wavelet neural network in this paper.

(2) *The Number of Wavelet Units.* At present, there is no theoretical guidance about choosing the number of wavelet units in hidden layer [25]. However, there are lots of empirical formulas, and they can be expressed as

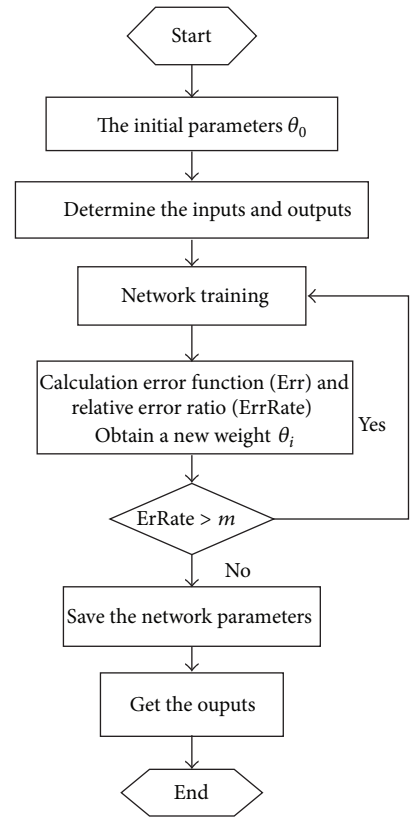

Figure 2: The flow chart of wavelet neural network. Note: θ_0 and θ_i are the network parameters matrices and m is determined by the owner's requests.

$$l = \sqrt{m \times n} \tag{6a}$$

$$l = \sqrt{m + n} + t \tag{6b}$$

$$l = \sqrt{0.43mn + 0.12n^2 + 2.54\,m + 0.77n + 0.35} + 0.51 \tag{6c}$$

$$l = \frac{mn + (1/2)\, n\left(n^2 + n\right) - 1}{m + n}, \tag{6d}$$

where n is the number of input nodes, m is the number of output nodes, and t is a constant between 1 and 20.

Theoretically, there should be an optimal number of wavelet units in hidden layer. However, these empirical formulas are always gained from experiments in other fields, and they can only get a range or approximation instead of an exact figure. Therefore, the experience formulas can only be taken as a reference to determine the number of wavelet units in hidden layer in the field of civil engineering.

(3) *Parameters Initialization of Wavelet Neural Network.* As an example, l is the number of nodes in hidden layer, n is the number of nodes in input layer, w_{ki} is the weight parameters between the kth neuron of hidden layer and the ith neuron of input layer, and ν_k is weight parameters between the kth

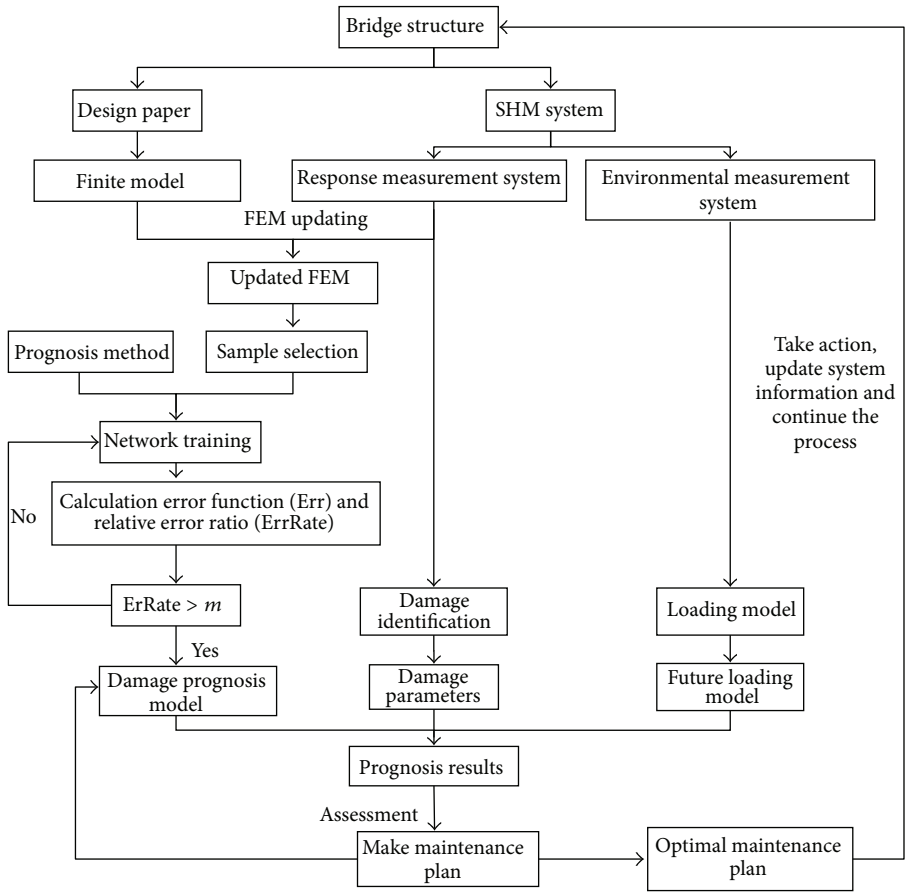

Figure 3: A general damage prognosis solution procedure based on wavelet neural network and model updating.

Table 1: Comparison of updated frequencies and measured frequencies, MAC values (unit, Hz).

Model number	Measured frequencies ①	Updated frequencies ②	Relative error (② − ①)/① (%)	MAC values (%)
beam-0				
First order	33.62	32.78	−2.5	93.1
Second order	135.03	130.78	−3.1	91.4
Third order	293.03	293.02	0	95.5
beam-1				
First order	20.71	22.02	6.3	95.1
Second order	131.02	130.04	−0.7	93.4
Third order	231.18	232.69	−0.7	90.9
beam-2				
First order	18.90	19.46	2.9	96.7
Second order	85.94	90.67	5.5	94.3
Third order	202.54	203.07	0.3	90.8
beam-3				
First order	17.02	17.29	1.6	94.7
Second order	66.69	67.14	0.7	94.9
Third order	148.33	149.68	0.9	90.2

Table 2: Training samples of the experimental design.

N	Inputs of section stiffness ($\times 10^{-6}$ m^4)			Output of the fundamental frequency (Hz)
	Damage section-1	Damage section-2	Damage section-3	
1	0.93	0.92	2.2	30.67
2	0.05	0.05	1.58	14.07
3	1.21	1.4	0.45	29.91
⋮	⋮	⋮	⋮	⋮
28	0.05	2.23	0.72	20.18
29	0.05	0.73	2.23	19.91
30	0.05	0.05	0.05	12.56

Table 3: The test samples.

N	Inputs of section stiffness ($\times 10^{-6}$ m^4)			Outputs of fundamental frequency (Hz)
1	2.23	0.105	2.23	22.018
2	0.105	0.105	2.23	19.455
3	0.105	0.105	0.105	17.288

Note: "N" is the number of the samples.

Table 4: The results of damage prognosis.

N	The measured values f_0	Theoretical values f_1	Output values f_2	The error rate with theoretical values $\lvert(f_2 - f_1)/f_1\rvert$	The error rate with measured values $\lvert(f_2 - f_0)/f_1\rvert$
1	20.713	22.018	21.72	1.35%	4.86%
2	18.903	19.455	19.59	0.70%	3.63%
3	17.017	17.288	16.76	3.02%	–1.51%

Table 5: Parameters change before and after updating based on the response surface method.

Updated parameters	E_0 ($\times 10^4$ MPa)	E_1 ($\times 10^4$ MPa)	E_2 ($\times 10^4$ MPa)	E_3 ($\times 10^4$ MPa)	K_1 ($\times 10^6$ N/m)	K_2 ($\times 10^6$ N/m)	K_3 ($\times 10^6$ N/m)
2012	3.6	3.5	3.2	2.5	0.6	3.1	3.1
2013	3.3	2.8	3.2	2.2	0.9	4.7	1.7
Rate (%)	−8.8	−19.8	−1.9	−12.4	50.0	48.4	−43.3

Notice: E_1 is the elasticity modulus of webs in the 2nd, 3rd, and 5th spans; E_2 is the elasticity modulus of web in the 4th span; E_3 is the elasticity modulus of bottom slab in the 2nd, 5th spans; E_0 is the elasticity modulus of the other parts; K_1 is transverse spring stiffness at the support and expansion joints; K_2 is the longitudinal spring stiffness at the support; K_3 is the longitudinal spring stiffness at the expansion joints.

Table 6: Comparison of updated frequencies and measured frequencies (unit, Hz).

Vibration mode	Frequency (Hz)					
	Measured value-1 (SSI)	Updated value-1	Error-1 (%)	Measured value-2 (SSI)	Updated value-2	Error-2 (%)
Vertical						
First order	2.89	2.88	0.43	2.87	2.77	3.48
Second order	3.03	3.081	1.84	3.16	2.89	8.66
Third order	3.79	3.61	0.51	3.67	3.34	8.99
Fourth order	4.26	4.32	1.27	4.25	4.02	5.37
Transverse						
First order	0.83	0.73	0.16	0.92	0.87	4.90
Second order	1.43	1.47	2.84	1.45	1.48	1.45
Longitudinal						
First order	1.79	1.74	2.45	1.30	1.28	1.61

Notice: measured value-1, updated value-1, and error-1 were the updated results in February 2012; measured value-2, updated value-2, and error-2 were the updated results in June 2013.

Table 7: Training samples.

N	E_0 ($\times 10^4$ MPa)	E_1 ($\times 10^4$ MPa)	E_2 ($\times 10^4$ MPa)	E_3 ($\times 10^4$ MPa)	Vehicle load F	The maximum value of displacement	The maximum value of strain
1	2.5	1.5	2	1.5	2.0	35.700	443.51
2	2.5	3.3	2	3	2.0	28.316	347.75
⋮	⋮	⋮	⋮		⋮	⋮	⋮
30	3.5	1.5	2.6	1.5	1.1	16.164	198.27
31	2.5	3.3	3.5	1.5	2.0	28.969	352.76

Notice: the value of vehicle load (F) is the n times of highway-I load.

Table 8: Verification of the results of damage prognosis model.

Measure value	Measured values	Outputs of network	Error (%)
The maximum value of displacement (mm)	15.37	16.77	9.11
The maximum value of strain ($\mu\varepsilon$)	534	475.2	11.01

neuron of hidden layer and the unit of output layer. Initial parameters of w_{ki}, ν_k, a_k, b_k can be obtained by the experiential analysis of signals; reasonable parameters can reduce the number of iterations; however, the empirical formulas have not been verified widely. Compared with the circulation signals in mechanical engineering, the measured signals from real civil engineering structures are more discrete and stochastic, so initial parameters cannot be defined as those from mechanical engineering [26, 32, 35]. The empirical formulas have been tried to select the initial parameters, but the results are not satisfactory. It is not easy to describe a parameter which contains discreteness and randomness by a deterministic formula. A standard normal distribution random matrix is herein used as the initial parameters; the results were conformed to be accurate and effective.

3. The Framework of Damage Prognosis Based on Wavelet Neural Network and Model Updating

Damage prognosis combines model-based method with date-driven method. Namely, the structural responses are calculated based on the updated finite element model and used as sample values which are needed by data-driven method [2–4]. Thus, the advantages of the two methods can be combined effectively in order to get a suitable DP model. It can be applied to evaluate the structure safety and to put forward the best maintenance plan. The basic process is shown in Figure 3. The process begins by collecting as much initial system information as possible. This information is used to develop model-based numerical model of the structure as well as to define the system that will be used for state awareness assessments and whatever sensors needed to monitor operational and environment conditions. As the data become available from the SHM system, they will be used to validate and update the FE model, and the updated and validated model can be used to develop the DP model based on the wavelet neural network method, which is the key part of the framework; the other part is damage identification, where the data of SHM system will also be used to assess the current state of the structure (existence, location, type, and extent of damage). Data from the operational and environmental sensors will be used to predict the future system loading. The output of the future loading model, state awareness model, and the DP model will be used to estimate the future state of the structure. As is indicated, the solution process will be iterative, relying on experience gained from past predictions to improve future predictions.

4. Damage Prognosis of Steel Beam Model

At present, there are rarely experiments about DP in the field of civil engineering. In this paper, through a damaged I-steel beam model testing, the damage evolution of the dynamic property is explored. Finally, the prediction results based on the wavelet neural networks method are compared with the ambient vibration testing results in order to verify the validity of the proposed DP method.

4.1. The Model Testing. This testing includes four I-steel beams, each one with a length of 3 meters. The density of the steel material is 7800 kg/m^3, and the elasticity modulus is 2.1×10^5 MPa. In the I-section, area is 14.33 cm^2, inertia moment is 223 cm^4, and the damage section inertia moment is 10.5 cm^4. Among the four beams in this testing, one beam is undamaged, marked as beam-0; one has a notch in the $L/2$ of the beam, marked as beam-1; one has two notches in the $L/2$ and the $L/4$ of the beam, marked as beam-2; and the last one has 3 notches in the middle, a quarter, and 3 quarters of the beam, marked as beam-3. The notches of the beams got the same length of 0.1 m and a height of 0.05 m (half of the beam height) (Figure 4). The ambient vibration testing of beam-2 is shown in Figure 5; data was sampled at 1000 Hz, and each setup for all tests was recorded for duration of 15 minutes. The vertical frequencies can be obtained by testing, as shown in Table 1.

Figure 4: The notch of steel beam.

Figure 5: The environmental vibration testing.

4.2. The Finite Element Model Updating of Steel Beam. Using ANSYS finite element (FE) analysis software, these FE beam models are established by beam-3 elements, and it is composed of 60 elements and 61 nodes, as shown in Figure 6. The first three order frequencies are selected as the response features; I_1, I_2, and I_3 are the inertia moment of damage elements in the middle, a quarter, and 3 quarters of the beam. Then FE model updating is conducted based on third-order response surface method [36], and the updated frequencies, measured frequencies, and MAC values are shown in Table 1.

4.3. Determine the Network Structure and Initial Parameters. Wavelet neural network training is conducted according to the method of this paper, and Morlet wavelet is selected as the excitation function; the network training is effective when the number of wavelet units in hidden layer is 3 (as (6b), $l = \sqrt{3+1}+1 = 3$, and $t = 1$), the number of training is set as 10000 times, error $m = 0.001$, and the training rate $\alpha = \beta = 0.01$; $\gamma = \eta = 0.001$.

According to the standard normal distribution, the initial parameters are selected randomly as follows:

$$W = \begin{Bmatrix} -0.824 & 2.288 & -0.852 \\ 1.874 & 0.375 & 0.072 \\ -4.427 & -1.939 & 4.941 \end{Bmatrix};$$

$$V = \{1.125 \quad -1.352 \quad 3.647\}; \tag{7}$$

$$A = \{1.807 \quad -0.042 \quad 0.404\};$$

$$B = \{0.572 \quad -0.170 \quad 1.985\}.$$

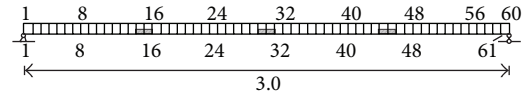

Figure 6: Numerical model (unit, m).

Note: "W," "V," "A," and "B" are the parameters of w_{ki}, ν_k, a_k, and b_k.

4.4. Wavelet Neural Network Training and Damage Prognosis Model. The future fundamental frequency of a damaged I-steel beam was selected as the output value in this paper. Firstly, the experimental samples were selected by D-optimal design method, and the damage degree was simulated by cutting section stiffness. Then fundamental frequencies of beams under different damage degrees were calculated through the updated FE model. In order to validate the network, three beams were employed as the test samples, as shown in Tables 2 and 3.

The training samples and test samples are put into the wavelet neural networks solution procedure based on MATLAB 7.0 software. Then adaptive training was realized, and suitable weight parameters can be obtained. Furthermore, the DP function model can be established.

4.5. The Result of Damage Prognosis. As the DP function model has been established, the fundamental frequencies of these three steel beams can be predicted relying on the function model. The DP results based on wavelet neural network are shown in Table 4. It is shown that the predicted results based on wavelet neural network and the measured results from model testing are very well consistent, and the error is less than 5%.

5. Damage Prognosis Analysis of Xinyihe Bridge

5.1. Engineering Background. Xinyihe Bridge (Figure 7) of the Beijing-Shanghai Highway is located in Shuyang, Jiangsu province. The upper structure is a six-span continuous beam bridge, and design loads are car-super level 20 and trailer-120. It was built in 2001 and has served for 12 years.

5.2. Load Prediction. The traffic data used were monthly average number of cars during June 2012 to June 2013 (Figure 8); the DP model based on wavelet neural network method could provide short-term predictive traffic information (one month). According to the historical traffic data, it is obvious that the traffic intensity in a given month (n) is related to the last 3 months' (n-1, n-2, and n-3) traffic intensity (Q_{n-1}, Q_{n-2}, and Q_{n-3}) and the given month (n), so the 4 parameters (Q_{n-1}, Q_{n-2}, Q_{n-3}, and n) could be the input values, and the traffic intensity Q_n will be the output value. Based on the wavelet neural network method and the traffic data, the traffic intensity prediction could be realized. As shown in Figures 8 and 9, within the next year and a half, the traffic intensity will increase and seasonal differences will decrease; the prediction

(a) Xinyihe Bridge panorama photo (b) The weigh-in-motion (WIM)

Figure 7: Xinyihe Bridge.

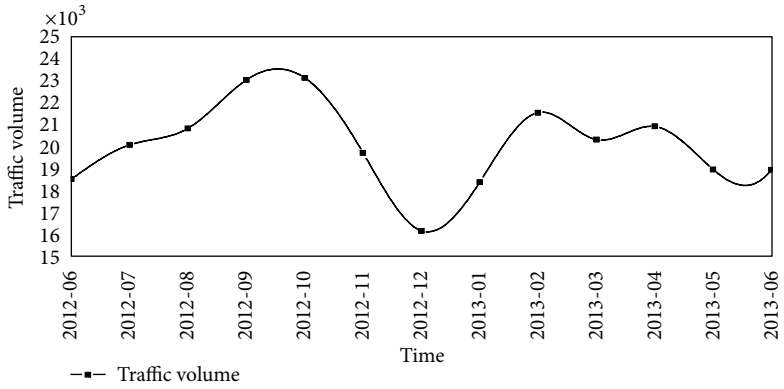

Figure 8: Historical traffic intensity (2012.06–2013.06).

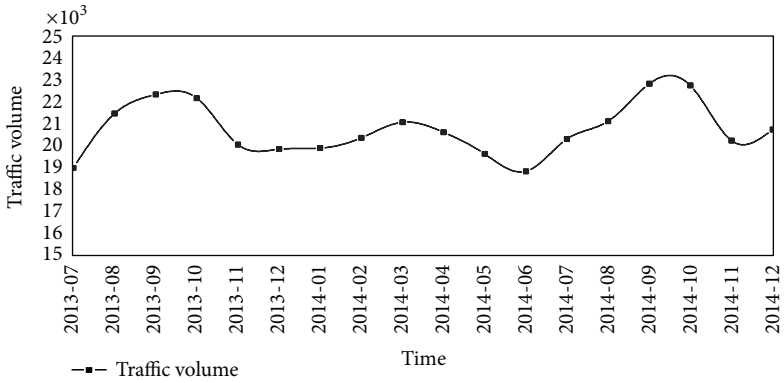

Figure 9: The future traffic intensity (2013.07–2014.12).

Figure 10: The static and dynamic test of Xinyihe Bridge.

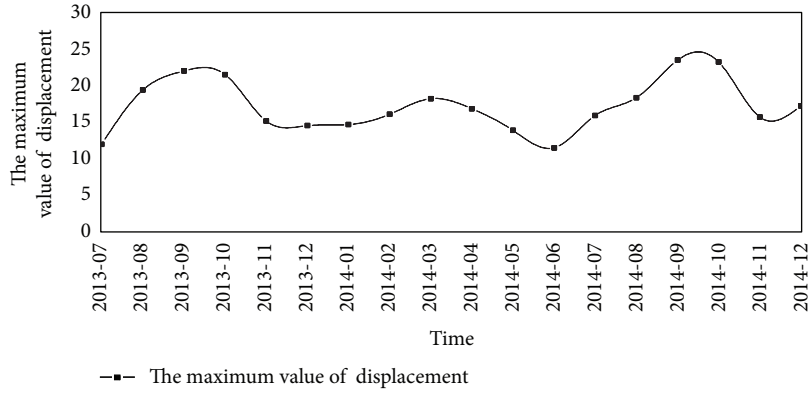

Figure 11: The maximum value of displacement (2013.07–2014.12).

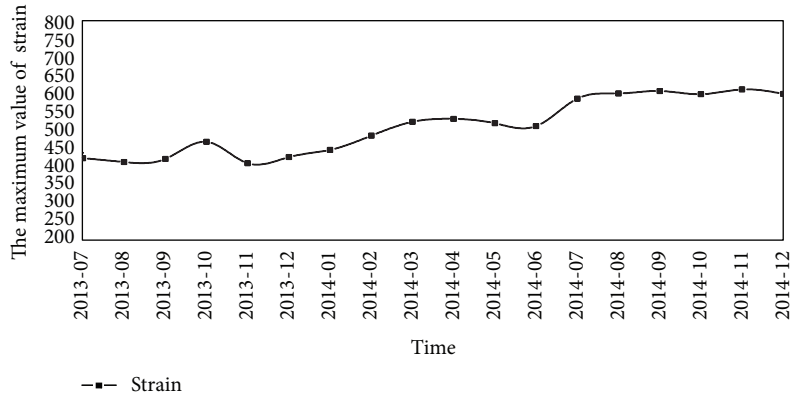

Figure 12: The maximum value of strain (2013.07–2014.12).

model can be employed for the bridge safety evaluation of Beijing-Shanghai Highway. As the WIM continues to collect the new data, the samples will be refreshed constantly, and the load prediction model could be updated continuously.

5.3. The Model Updated of Xinyihe Bridge. According to the design papers, the FE model was built. Based on the twice ambient vibration testing in 2012 and 2013, the FE model was updated according to the third-order response surface method [36]. The updated frequencies are shown in Table 5, and the updated parameters are shown in Table 6.

As mentioned above, the FE model could be updated continuously based on the results of ambient vibration testing in the future. If there are enough frequencies samples, the wavelet neural network will be used for the model parameters prediction, namely, the prediction of the FE model. Due to that there is no real-time dynamics monitoring, we could not have enough samples, and then the model parameters change rate between the two updated FE models will be used as the actual structure performance degradation rate in this paper.

5.4. The Damage Prognosis Model. The maximum values of displacement and strain were separately selected as outputs of the prognosis model in this paper, and the parameters (E_0, E_1, E_2, and E_3) and load (F) were selected as the inputs. Similarly to the previously damaged I-steel beams, the parameters samples were selected by D-optimal design method, and the training samples could be obtained based on the finite element analysis model, as shown in Tables 7 and 8.

The training samples are substituted into the MATLAB model based on wavelet neural network; the DP model can be established relying on the self-training of the prognosis model, and the goal is the error parameter $E < m$.

5.5. Validation and Application of Prognosis Results. The accuracy of the prognosis model is verified by comparing the prediction results with the static test results in June 2013, as shown in Figure 10. The maximum values of displacement and strain under highway-I load can be obtained based on the static test, and this damage degree is similar to the state of the second ambient vibration test. The results were compared with the prognosis results based on wavelet neural network, as shown in Table 8. It is clear that the prediction results of DP and the measured results of static test are very well consistent, and the errors of the maximum values of displacement and strain are less than 12% (seen in Table 8).

As shown in Table 8, the DP model can be used in the bridge health monitoring system, and then based on the load prognosis model and the updated model, the maximum values of displacement and strain under working load conditions

can be predicted from July 2013 to December 2014, as shown in Figures 11 and 12. The results show that the traffic volume will increase and seasonal differences will decrease in the next year and a half; the displacement has a slight increase and seasonal characters in the critical section of mid span, but the strain increases distinctly, and timely remedial actions need to be taken.

6. Conclusions

(1) A damage prognosis framework for bridge structure is proposed combining the wavelet neural network method with the finite element model updating. The effectiveness of the proposed method is verified through a damaged I-section steel beam testing, and the maximum error is less than 5%.

(2) The prognosis method can be used to predict future traffic load volume based on the traffic load monitoring. The traffic intensity predictions of Xinyihe Bridge show that the traffic volume will increase and seasonal differences will decrease in the next year and a half.

(3) The prognosis prediction results agree very well with those from static load testing of Xinyihe Bridge. The errors between the predicted and measured results were within the range of 12%. The displacement has slight seasonal characters in the mid span, and the strains increase distinctly. The prognosis model can be used for the bridge safety prognosis and future maintenance.

(4) This paper only solves the problem of the predicting of the future structural loads and structural properties. The remaining life prediction of real bridge structure is the next attention of our research. The proposed damage prognosis method can be incorporated into the structure health monitoring system, for the purpose of the online safety prognosis, and cost-efficient condition based maintenance of bridge structures.

Conflict of Interests

The authors declare that there is no conflict of interests regarding the publication of this paper.

Acknowledgments

The authors gratefully acknowledge the financial support provided by the Natural Science Foundation Committee of China (Grant nos. 51178101 and 51378112) and the University Graduate Student Scientific Research Innovation Plan of Jiangsu Province (Grant no. CXZZ13_0109).

References

[1] J. Ou and H. Li, "Structural health monitoring in mainland china: review and future trends," *Structural Health Monitoring*, vol. 9, no. 3, pp. 219–231, 2010.

[2] C. R. Farrar, H. Sohn, F. M. Hemez et al., "Damage prognosis: current status and future needs," Los Alamos National Laboratory Report LA-14051-MS, 2003.

[3] D. J. Inman, C. R. Farrar, V. L. Junior, and V. S. Junior, *Damage Prognosis for Aerospace, Civil and Mechanical Systems*, John Wiley & Sons, London, UK, 2005.

[4] C. R. Farrar and N. A. J. Lieven, "Damage prognosis: the future of structural health monitoring," *Philosophical Transactions of the Royal Society A: Mathematical, Physical and Engineering Sciences*, vol. 365, no. 1851, pp. 623–632, 2007.

[5] B. Terry and S. Lee, "What is the prognosis on your maintenance program," *Engineering and Mining Journal*, vol. 5, pp. 102–111, 1995.

[6] H. Li, D. Tao, Y. Huang, and Y. Bao, "A data-driven approach for seismic damage detection of shear-type building structures using the fractal dimension of time-frequency features," *Structural Control and Health Monitoring*, vol. 20, no. 9, pp. 1191–1210, 2013.

[7] W. L. Oberkampf and C. J. Roy, *Verification and Validation in Scientific Computing*, Cambridge University Press, New York, NY, USA, 2011.

[8] A. Heng, S. Zhang, A. C. C. Tan, and J. Mathew, "Rotating machinery prognostics: state of the art, challenges and opportunities," *Mechanical Systems and Signal Processing*, vol. 23, no. 3, pp. 724–739, 2009.

[9] C. Ding, J. Xu, and L. Xu, "ISHM-based intelligent fusion prognostics for space avionics," *Aerospace Science and Technology*, vol. 29, no. 7, pp. 200–205, 2013.

[10] M. Gobbato, J. P. Conte, J. B. Kosmatka, and C. R. Farrar, "A reliability-based framework for fatigue damage prognosis of composite aircraft structures," *Probabilistic Engineering Mechanics*, vol. 29, pp. 176–188, 2012.

[11] J. H. Luo, K. R. Pattipati, L. Qiao, and S. Chigusa, "Model-based prognostic techniques applied to a suspension system," *IEEE Transactions on Systems, Man, and Cybernetics A:Systems and Humans*, vol. 38, no. 5, pp. 1156–1168, 2008.

[12] Y. J. Luo, Z. Kang, and A. Li, "Structural reliability assessment based on probability and convex set mixed model," *Computers and Structures*, vol. 87, no. 21-22, pp. 1408–1415, 2009.

[13] M. A. Caminero, S. Pavlopoulou, and M. Lopez-Pedrosa, "Analysis of adhesively bonded repairs in composites: damage detection and prognosis," *Composite Structures*, vol. 95, no. 3, pp. 500–517, 2013.

[14] B. A. Zárate, J. M. Caicedo, J. Yu, and P. Ziehl, "Bayesian model updating and prognosis of fatigue crack growth," *Engineering Structures*, vol. 45, pp. 53–61, 2012.

[15] J. He, Z. Lu, and Y. Liu, "New method for concurrent dynamic analysis and fatigue damage prognosis of bridges," *Journal of Bridge Engineering*, vol. 17, no. 3, pp. 396–408, 2012.

[16] S. S. Kulkarni and J. D. Achenbach, "Structural health monitoring and damage prognosis in fatigue," *Structural Health Monitoring*, vol. 7, no. 1, pp. 37–49, 2008.

[17] R. B. Chinnam and P. Mohan, "Online reliability estimation of physical systems using neural networks and wavelets," *International Journal of Smart Engineering System Design*, vol. 4, no. 4, pp. 253–264, 2002.

[18] C. Chen, D. Brown, C. Sconyers, B. Zhang, G. Vachtsevanos, and M. E. Orchard, "An integrated architecture for fault diagnosis and failure prognosis of complex engineering systems," *Expert Systems with Applications*, vol. 39, no. 10, pp. 9031–9040, 2012.

[19] M. Gobbato, J. B. Kosmatka, and J. P. Conte, "A recursive Bayesian approach for fatigue damage prognosis: an experimental validation at the reliability component level," *Mechanical Systems and Signal Processing*, vol. 45, no. 2, pp. 448–467, 2014.

[20] M. Rabiei and M. Modarres, "A recursive Bayesian framework for structural health management using online monitoring and periodic inspections," *Reliability Engineering and System Safety*, vol. 112, pp. 154–164, 2013.

[21] Y. Lei, Y. Jiang, and Z. Xu, "Structural damage detection with limited input and output measurement signals," *Mechanical Systems and Signal Processing*, vol. 28, pp. 229–243, 2012.

[22] Y. Lei, C. Liu, Y. Q. Jiang, and Y. K. Mao, "Substructure based structural damage detection with limited input and output measurements," *Smart Structures and Systems*, vol. 12, no. 6, pp. 619–640, 2013.

[23] S. Amin, C. Byington, and M. Watson, "Fuzzy inference and fusion for health state diagnosis of hydraulic pumps and motors," *Journal of Vibration and Control*, vol. 7, no. 15, pp. 13–18, 2009.

[24] X. Guan, R. Jha, and Y. Liu, "Model selection, updating, and averaging for probabilistic fatigue damage prognosis," *Structural Safety*, vol. 33, no. 3, pp. 242–249, 2011.

[25] X. Guan, R. Jha, and Y. Liu, "Probabilistic fatigue damage prognosis using maximum entropy approach," *Journal of Intelligent Manufacturing*, vol. 23, no. 2, pp. 163–171, 2012.

[26] Q. Zhang, "Using wavelet network in nonparametric estimation," *IEEE Transactions on Neural Networks*, vol. 8, no. 2, pp. 227–236, 1997.

[27] N. Catbas, H. B. Gokce, and D. M. Frangopol, "Predictive analysis by incorporating uncertainty through a family of models calibrated with structural health-monitoring data," *Journal of Engineering Mechanics*, vol. 139, no. 6, pp. 712–723, 2013.

[28] P. Nie, X. Chen, T. Xu, and B. Sun, "State recognition of tool wear based on wavelet neural network," *Journal of Beijing University of Aeronautics and Astronautics*, vol. 37, no. 1, pp. 106–109, 2011 (Chinese).

[29] L. Liu and Y. Yang, "Fault diagnostics system for helicopter main gearbox using wavelet neural network," *Journal of Aerospace Power*, vol. 27, no. 6, pp. 1255–1260, 2012 (Chinese).

[30] J. Fan, *The Basic Principles and Methods of Intelligent Neural Calculation*, The Southwest Jiao tong University Press, Chengdu, China, 2000 (Chinese).

[31] Y. Oussar and G. Dreyfus, "Initialization by selection for wavelet network training," *Neurocomputing*, vol. 34, pp. 131–143, 2000.

[32] L. Yang, *Research on Wavelet Process Neural Network Correlative Theory and Its Application*, Harbin Institute of Technology, Harbin, China, 2008 (Chinese).

[33] M. J. Shensa, "The discrete wavelet transform: wedding the atrous and mallat algorithms," *IEEE Transactions on Signal Processing*, vol. 40, no. 10, pp. 2464–2482, 1992.

[34] M. J. Shensa, "Discrete inverses for nonorthogonal wavelet transforms," *IEEE Transactions on Signal Processing*, vol. 44, no. 4, pp. 798–807, 1996.

[35] S. Zhong, Y. Li, G. Ding, and L. Lin, "Continuous wavelet process neural network and its application," *Neural Network World*, vol. 17, no. 5, pp. 483–495, 2007 (Chinese).

[36] Z. Zong, F. Chu, and J. Niu, "Damage identification methods using response surface based finite element model updating of bridge structures," *China Civil Engineering Journal*, vol. 46, no. 2, pp. 115–122, 2013 (Chinese).